HYDROMAGNETIC FLOW OF A CARREAU FLUID IN A CURVED CHANNEL WITH NON-LINEAR THERMAL RADIATION

by

Zaheer ABBAS[a], Muhammad IMRAN[a], and Muhammad NAVEED[b*]

[a] Department of Mathematics, The Islamia University of Bahawalpur, Bahawalpur, Pakistan
[b] Department of Mathematics, Khwaja Fareed University of Engineering & Information Technology, Rahim Yar Khan, Pakistan

Original scientific paper
https://doi.org/10.2298/TSCI171011077A

The study depicts the variations in the hydromagnetics flow of a Careau fluid in a semi permeable curved channel with convective boundary condition. Furthermore, Rosseland approximation is also considered to analyze the non-linear thermal radiation effects. Curvilinear co-ordinates system has been adopted for the mathematical modeling of the flow equations. The attained set of governing equation are then converted into non-linear dimensionless differential equations, by making use of similarity variables which are later treated by shooting method. In addition, the Newton's Raphson method is also incepted to improve the accuracy of the obtained numerical result. The velocity field and temperature distributions are affected by various involved parameter which are presented in graphs and in table form. It is noticed that the velocity profiles are influenced by the change in the Weissenberg number

Key words: *semi porous curved channel, Carreau fluid, convective boundary condition, non-linear thermal radiation*

Introduction

Flow analysis in a semi-porous or porous channel or tubes obtained considerable attention in the last few years because of its large number of utilization in the arena of biomedical and mechanical engineering, which consists of flow in blood oxygenators, manufacturing of porous or semi-porous pipes, flow of blood in capillaries, design of filter and dialysis of blood in synthetic kidney. The analysis of flow behavior in the channel was initiated by Berman [1], and gave the exact solution of the flow equations. Analysis of flow done by [1] was extended in diverse directions by several researchers to discuss the varied aspects of flow for both viscous and non-Newtonian fluids. For more details, the interested readers are directed to the articles [2-7] and many references therein.

The analysis of magnetic field along with the thermal radiation in the heat exchange flow problems are crucial in process involving high temperature for example storage of thermal energy, turbine, nuclear power plant, solar power technology, electrical power era, space vehicle re-entry and many others. In the couple of papers Pantokratoras and Fang [8, 9] investigate the non-linear thermal radiation effects on the viscous fluid both for Sakiadis and Blasius flow respectively. The examination of the convective heat transfer flow on the stretching wall with non-linear thermal radiation was done by Cartel [10]. Kumar *et al.* [11] discussed the effects

* Corresponding author, e-mail: rana.m.naveed@gmail.com

of non-linear thermal radiation on Williamson fluid on a stretching surface. Mushtaq *et al.* [12] analyzed the impacts of non-linear thermal radiation on the flow of nanofluid. A glance at the recently published literature shows that various aspects of convective heat transfer flow with magnetic field and thermal radiation have been investigated by several researchers [13-23].

The investigation of flow characteristics of non-Newtonian fluids has acquired significant importance due to its extensive scope of utilization in chemical engineering and industrialized process, for example molten of plastics, properties of paint and blood. In aforesaid problems, the fluid's rheology is intensely complicated, since at any point during the flow motion the apparent viscosity of the fluid developed into a relation between a shear stress and the local shear rate, and several flow models for non-Newtonian fluid have been formulated to characterize such flow behaviors. A good example of such flow models are the Carreau model [24], power law model, Maxwell fluid model for pseudoplastic and dilatant fluid, Casson and Herschel-Bulkley model for viscoelastic fluid [25]. The impacts of transferring of heat in MHD flow of a viscoelastic fluid through a channel by considering oscillatory starching surface was examined by Missra *et al.* [26]. Hsiao [27] investigated the influence of magnetic and viscous dissipation effects on a micropolar nanofluid flow on a stretching sheet. Hayat *et al.* [28] examined the impacts of heat exchange processes on a hydromantic flow of an upper convected Maxwell fluid through a channel in a permeable medium. The study of heat exchange in a hydromagnetic flow of a viscoelastic fluid past a channel was done by Raftari and Vajravelu [29]. They obtained the analytic solution of the problem by using Homotopy perturbation technique. Abbas *et al.* [30] examined the hydrodynamic flow of non-Newtonian fluid through a semi permeable channel. Recently, Masood *et al.* [31] investigated the impacts of magnetic field and non-linear thermal radiation on Carreau fluid.

On the other side, the review of literature points out that the research and information is scarce for the flow through a curved channel. The study of flow in a camped curved channel has gotten a great deal of attention because of its so many utilization in an arena of biological and engineering processes. Khuri [32] studied the Stoke's flow through the curved channel. Fu *et al.* [33] examined the impacts of forced convection on the flow of a reciprocating curve channel embedding in a permeable medium. Naveed *et al*. [34] examined the impacts of porosity and radiation on the flow of viscous fluid through a semi permeable curved shape channel. The impacts of Hall current with non-linear radiation on the flow of viscous fluid through a curved shape channel was analyzed by Abbas *et al.* [35]. Sajid *et al.* [36] analyzed the impacts of magnetic field and Joule heating on a nanofluid flow past a semi permeable curved shape channel.

The objective of the existing study is to examine the impacts of applied external magnetic field with non-linear radiative heat exchange in a Carreau fluid flowing in a semi permeable curved channel in which lower wall of the channel is convectively heated. Numerical solutions of the resulting equations are obtained by employing shooting method and impacts of diverse parameters are illustrated through graphs and table.

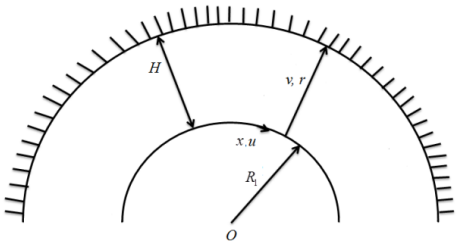

Figure 1. Physical model and co-ordinate system

Presentation of the problem

Consider 2-D and incompressible boundary-layer hydromagnetic flow of a Carreau fluid through a semi permeable curved channel separated by a distance, H, curled in a round circle of radius, R_1, fig.1. Moreover, the lower surface of the channel is rigid, whilst the upper wall is perme-

able on which a non-Newtonian fluid is injected. It is assumed that the temperature of the lower wall is T_1 which is kept fixed by employing convective boundary condition and the temperature of the upper wall is assumed as T_0 with $T_1 > T_0$. In addition, a uniform magnetic field of intensity B_0 is incorporated in r-direction. By these assumptions, continuity, momentum and energy equations for the flow of Carreau fluid are:

$$\frac{\partial}{\partial r}\left[\left(r+R_1\right)w\right]+R_1\frac{\partial z}{\partial x}=0 \tag{1}$$

$$\frac{z^2}{r+R_1}=\frac{1}{\rho}\frac{\partial p}{\partial r} \tag{2}$$

$$w\frac{\partial z}{\partial r}+\frac{zR_1}{r+R_1}\frac{\partial z}{\partial x}+\frac{zw}{r+R_1}=-\frac{1}{\rho}\frac{R_1}{r+R_1}\frac{\partial p}{\partial x}-\frac{\sigma}{\rho}B_0^2z+$$
$$+\nu\left\{\left[1+\lambda_1^2\left(\frac{\partial z}{\partial r}-\frac{z}{r+R_1}\right)^2\right]^{\frac{n-1}{2}}+\left(n-1\right)\lambda_1^2\left(\frac{\partial z}{\partial r}-\frac{z}{r+R_1}\right)^2\left[1+\lambda_1^2\left(\frac{\partial z}{\partial r}-\frac{z}{r+R_1}\right)^2\right]^{\frac{n-3}{2}}\right\}\cdot$$
$$\cdot\left(\frac{\partial^2 z}{\partial r^2}+\frac{1}{r+R_1}\frac{\partial z}{\partial r}-\frac{z}{\left(r+R_1\right)^2}\right) \tag{3}$$

$$w\frac{\partial T}{\partial r}+\frac{R_1 z}{\left(r+R_1\right)}\frac{\partial T}{\partial x}=\alpha^*\left[\frac{\partial^2 T}{\partial r^2}+\frac{1}{\left(r+R_1\right)}\frac{\partial T}{\partial r}\right]-\frac{1}{\left(r+R_1\right)}\frac{\partial}{\partial r}\left(r+R_1\right)q_r \tag{4}$$

In previous equations w and z denote the velocity components along the r and x-directions, respectively, and λ_1, α^*, q_r, ν, T, n, p, and ρ are the relaxation time, thermal diffusivity, radiative heat flux, kinematic viscosity, temperature, power law index, pressure, and density of the fluid, respectively.

The suitable boundary conditions to present the flow and heat transfer are [34]:

$$\left.\begin{aligned} &z=v_s,\ \ w=0,\quad -k\frac{\partial T}{\partial r}=h_f\left(T_1-T\right),\ \ \text{at } r=0\\ &z=0,\ \ w=\frac{-v_sR_1}{r+R_1},\ \ T\to T_0,\qquad\qquad \text{at } r=H\end{aligned}\right\} \tag{5}$$

where $v_s<0$ is for injection velocity and $v_s>0$ represents the suction velocity, T_0 denote the temperature of the upper curved wall, h_f denote the convective heat transfer coefficient, and k denote the thermal conductivity of the fluid.

The radiative heat flux term is defined by Rosseland approximation as [37]:

$$q_r=-\frac{4\bar{\sigma}^*}{3\bar{k}^*}\frac{\partial T^4}{\partial r}=-\frac{16\bar{\sigma}^*}{3\bar{k}^*}T^3\frac{\partial T}{\partial r} \tag{6}$$

where $\bar{k}^*$ and $\bar{\sigma}^*$ are the mean absorption coefficient and Stefan-Boltzman constant, respectively.

The dimensionless temperature field is given [35]:

$$\theta(\bar{\xi}) = T - \frac{T_0}{T_1} - T_0 \text{ along with } T = T_0\left[\left(\theta_w - 1\right)\theta\left(\bar{\xi}\right) + 1\right] \tag{7}$$

and $\theta_w = T_1/T_0$ indicates the temperature parameter.

Invoking eqs. (6) and (7) in energy eq. (4), one can obtain:

$$w\frac{\partial T}{\partial r} + \frac{zR_1}{r+R_1}\frac{\partial T}{\partial x} = \frac{\alpha^*}{(r+R_1)}\frac{\partial}{\partial r}\left(\left\{1 + Rd\left[\theta\left(\theta_w - 1\right) + 1\right]^3\right\}(r+R_1)\frac{\partial T}{\partial r}\right) \tag{8}$$

where $Rd = 16\bar{\sigma}^* T_\infty^3 / 3\bar{k}^* k$ is termed as a radiation parameter.

Similar solutions of the governing equations are obtained by employing the dimensionless transformations [34]:

$$z = \frac{v_s x}{H} f'(\bar{\xi}), \quad w = \frac{-R_1 v_s}{r+R_1} f(\bar{\xi}), \quad \bar{\xi} = \frac{r}{H}, \quad p = \frac{\rho v_s^2 x^2}{H^2} P(\bar{\xi}) \tag{9}$$

Introducing eq. (9), continuity eq. (1) is satisfied and eqs. (2), (3), and (8) yields:

$$\frac{\partial P}{\partial \bar{\xi}} = \frac{f'^2(\bar{\xi})}{\bar{\xi} + K_1} \tag{10}$$

$$\begin{aligned}
\frac{2K_1 \operatorname{Re} P}{\bar{\xi} + K_1} = {} & \left[1 + \operatorname{We}^2\left(\frac{f'}{\bar{\xi} + K_1} + f''\right)^2\right]^{\frac{n-3}{2}} \cdot \\
& \left\{\left[1 + n\operatorname{We}^2\left(\frac{f'}{\bar{\xi} + K_1} + f''\right)^2\right] f''' + \right. \\
& \left. + \left[1 + (2-n)\operatorname{We}^2\left(\frac{f'}{\bar{\xi} + K_1} + f''\right)^2\right]\left[\frac{f''}{\bar{\xi} + K_1} - \frac{f'}{\left(\bar{\xi} + K_1\right)^2}\right]\right\} + \\
& + \frac{\operatorname{Re} K_1}{\bar{\xi} + K_1} f f'' - \frac{\operatorname{Re} K_1}{\bar{\xi} + K_1} f'^2 + \frac{\operatorname{Re} K_1}{\left(\bar{\xi} + K_1\right)^2} f f' - \operatorname{Re} \mathrm{M}^2 f'
\end{aligned} \tag{11}$$

$$\frac{1}{\operatorname{Pr}\left(\bar{\xi} + K_1\right)}\left(\left\{1 + Rd\left[\theta\left(\theta_w - 1\right) + 1\right]^3\right\}\left(\bar{\xi} + K_1\right)\theta'\right)' + \frac{\operatorname{Re} K_1}{\bar{\xi} + K_1} f\theta' = 0 \tag{12}$$

where, $K_1 = R/H$, $\operatorname{Pr} = \mu c_p / k$, $\mathrm{M} = \sigma B_0^2 H / \rho U$, $\operatorname{We}^2 = \lambda_1^2 U^2 s^2 / H^4$, and $\operatorname{Re} = HU/\nu$ are the radius of curvature, Prandtl number, magnetic or Hartmann number, local Weissenberg number, Reynolds number, respectively.

Elimination of pressure term from the eqs. (10) and (11), one can obtain:

$$\left[1+\mathrm{We}^2\left(\frac{f'}{\bar{\xi}+K_1}+f''\right)^2\right]^{\frac{n-5}{2}}\cdot$$

$$\cdot\left\{\begin{array}{l}\left[1+\mathrm{We}^2\left(\frac{f'}{\bar{\xi}+K_1}+f''\right)^2\right]\left[1+n\,\mathrm{We}^2\left(f''+\frac{f'}{\bar{\xi}+K_1}\right)^2\right]\cdot\\ \cdot\left[f'''+\frac{f''}{\left(\bar{\xi}+K_1\right)^2}-\frac{f'}{\left(\bar{\xi}+K_1\right)^3}\right]+2\left[1+\mathrm{We}^2\left(f''+\frac{f'}{\bar{\xi}+K_1}\right)^2\right]^2\cdot\\ \cdot\left[\frac{f'''}{\bar{\xi}+K_1}-\frac{f''}{\left(\bar{\xi}+K_1\right)^2}+\frac{f'}{\left(\bar{\xi}+K_1\right)^3}\right]+\mathrm{We}^2\left[\begin{array}{l}f'''f''+\frac{f'''f'}{\bar{\xi}+K_1}+\\ +\frac{f''^2}{\bar{\xi}+K_1}-\frac{f'^2}{\left(\bar{\xi}+K_1\right)^3}\end{array}\right]\cdot\end{array}\right\}+$$

$$\cdot\left\{\left(n-1\right)\left\{\begin{array}{l}\left[3+n\,\mathrm{We}^2\left(f''+\frac{f'}{\bar{\xi}+K_1}\right)^2\right]f'''-\\ -\left[1+\left(n-2\right)\mathrm{We}^2\left(f''+\frac{f'}{\bar{\xi}+K_1}\right)^2\right]\end{array}\right\}\left[\frac{f''}{\bar{\xi}+K_1}-\frac{f'}{\left(\bar{\xi}+K_1\right)^2}\right]\right\}$$

$$+\frac{\mathrm{Re}\,K_1}{\bar{\xi}+K_1}\left(ff'''-ff''\right)+\frac{\mathrm{Re}\,K_1}{\left(\bar{\xi}+K_1\right)^2}\left(ff''-f'^2\right)-\frac{\mathrm{Re}\,K_1}{\left(\bar{\xi}+K_1\right)^3}ff'-\frac{\mathrm{Re}\,\mathrm{M}^2}{\bar{\xi}+K_1}f'-\mathrm{Re}\,\mathrm{M}^2f''=0 \tag{13}$$

Subjec to boundary conditions:

$$\begin{aligned}&f\left(\bar{\xi}\right)=f'\left(\bar{\xi}\right)-1=\theta'\left(\bar{\xi}\right)+\beta\left[1-\theta\left(\bar{\xi}\right)\right]=0 \quad \text{when } \bar{\xi}=0\\ &f\left(\bar{\xi}\right)-1=\ f'\left(\bar{\xi}\right)=\theta\left(\bar{\xi}\right)=0, \qquad\qquad\quad \text{when } \bar{\xi}=1\end{aligned} \tag{14}$$

The physical quantities of interests are the coefficient of skin-friction and the rate of heat transfer along the surface which are:

$$C_f=\frac{\tau_{rx}}{\rho U_w^2},\quad \mathrm{Nu}_s=\frac{xq_w}{k\left(T_w-T_0\right)} \tag{15}$$

In previoua equation q_w and τ_{rx} are the heat flux and shear stress at the surface in the x-directions, which are given:

$$\begin{aligned}&\tau_{rx}=\mu_0\left(\frac{\partial z}{\partial r}-\frac{z}{r+R_1}\right)\left[1+\lambda_1^2\left(\frac{\partial z}{\partial r}-\frac{z}{r+R_1}\right)^2\right]^{\frac{n-1}{2}}\Bigg|_{r=0}\\ &q_w=-k\frac{\partial T}{\partial r}\Bigg|_{r=0}+\left(q_r\right)_w\end{aligned} \tag{16}$$

Introducing eqs. (9) and (16), one can write eq. (15):

$$R_{ex}^{1/2}C_f = \left(f''(0)-\frac{1}{K_1}\right)\left[\mathrm{We}^2\left(f''(0)-\frac{1}{K_1}\right)^2+1\right]^{\frac{n-1}{2}}$$
$$R_{ex}^{-1/2}\,\mathrm{Nu}_x = -\left(Rd\theta_w^3+1\right)\theta'(0) \tag{17}$$

Numerical solution

The non-linear differential eqs. (12) and (13) with boundary conditions (14) are solved numerically by employing shooting method in the following way:

$$f' = y_1,\quad y_1' = y_2,\quad y_2' = y_3,$$
$$y' = \frac{-2\left[1+\mathrm{We}^2\left(y_2+\dfrac{y_1}{\xi+K_1}\right)^2\right]}{\left[1+n\,\mathrm{We}^2\left(y_2+\dfrac{y_1}{\xi+K_1}\right)^2\right]}\left[\frac{y_3}{\xi+K_1}-\frac{y_2}{(\xi+K_1)^2}+\frac{y_1}{(\xi+K_1)^3}\right]-$$
$$-\left[\frac{y_2}{(\xi+K_1)^2}-\frac{y_1}{(\xi+K_1)^3}\right]-\frac{\left[\begin{array}{l}\dfrac{\mathrm{Re}\,K_1}{\xi+K_1}\left(fy_3-y_1y_2\right)+\dfrac{\mathrm{Re}\,K_1}{(\xi+K_1)^2}\left(fy_2-y_1^2\right)-\\ -\dfrac{\mathrm{Re}\,K_1}{(\xi+K_1)^3}fy_1-\dfrac{\mathrm{Re}\,\mathrm{M}^2}{\xi+K_1}-\mathrm{M}^2\,\mathrm{Re}\,y_2\end{array}\right]}{\left[1+\mathrm{We}^2\left(y_2+\dfrac{y_1}{\xi+K_1}\right)^2\right]^{\frac{n-3}{2}}\left[1+n\,\mathrm{We}^2\left(y_2+\dfrac{y_1}{\xi+K_1}\right)^2\right]}- \tag{18}$$
$$-\frac{\mathrm{We}^2\left[y_2y_3+\dfrac{y_1y_3}{\xi+K_1}+\dfrac{y_2^2}{\xi+K_1}-\dfrac{y_1^2}{(\xi+K_1)^3}\right]}{\left[1+\mathrm{We}^2\left(y_2+\dfrac{y_1}{\xi+K_1}\right)^2\right]\left[1+n\,\mathrm{We}^2\left(y_2+\dfrac{y_1}{\xi+K_1}\right)^2\right]}\cdot$$
$$\cdot\left((n-1)\left\{\begin{array}{l}\left[3+n\,\mathrm{We}^2\left(y_2+\dfrac{y_1}{\xi+K_1}\right)^2\right]y_3-\\ -\left[1+(n-2)\,\mathrm{We}^2\left(y_2+\dfrac{y_1}{\xi+K_1}\right)^2\right]\end{array}\right\}\left[\frac{y_2}{\xi+K_1}-\frac{y_1}{(\xi+K_1)^2}\right]\right)$$

$$\theta' = g,\ g' = \frac{1}{1+\left[\theta(\theta_w-1)+1\right]^3 Rd}\left\{-3(\theta_w-1)\left[(\theta_w-1)\theta+1\right]^2 Rdg^2-\frac{K_1\,\mathrm{Re}\,\mathrm{Pr}}{\xi+K_1}fg\right\}-\frac{g}{\xi+K_1} \tag{19}$$

along with boundary conditions:

$$f(0)=0, \quad y_1(0)=1, \quad g(0)+\beta\left[1-\theta(0)\right]=0, \tag{20}$$

For simplicity of the flow equations we take $\xi=\overline{\xi}$. Integrating eqs. (18) and (19) as an initial value problem we need the values of $y_2(0)$ *i. e.* $f''(0)$, $y_3(0)$ *i. e.* $f'''(0)$ and $\theta'(0)$ *i. e.* $g(0)$, but we do not have such values. The initial presume values $f''(0)$, $f'''(0)$, and $g(0)$ are chosen and then integrated. The determined values of $f'(1)$ and $\theta(1)$ are equated with the given boundary conditions $f(1)=1$, $f'(1)=0$, and $\theta(1)=0$, and for better solution, the values of $f''(0)$, $f'''(0)$, and $g(0)$ are refined and adjusted by Newton Raphson's method. The step size has chosen as $\Delta\eta=0.01$. This process is repeated till the obtained results are converged inside the accuracy of 10^{-5} level.

Result and discussions

To highlight the impacts of different pertinent parameters on the fluid velocity, Nusselt number, skin friction coefficient, and temperature distribution, the graphical and tabular result are discussed here.

Figure 2 is displayed to see the analysis of velocity field, $f'(\xi)$, through the dimensionless radius of curvature, K_1. It is observed that the velocity field near the permeable surface decays for larger values of K_1, however after $\xi=4$ it starts increasing. Figure 3 demonstrates the variation of $f'(\xi)$ with magnetic parameter, M. It can be seen from this figure that the fluid velocity decays gradually for higher values of magnetic parameter, this behavior happens as a matter of fact that the magnetic field behaves as opposing force to the fluid motion. Figure 4 illustrates the influence of the Weissenburg number on $f'(\xi)$. It can be seen from the this figure that fluid velocity is increases for larger values of Weissenburg number. Figure 5 illustrates the variation on $f'(\xi)$ with several values of Reynolds number. It is noticed from this figure that velocity field is a decreasing function of Reynolds number. Figure 6 depicts the influence of power law index n, on the velocity field $f'(\xi)$, which exhibits that the fluid velocity is decreases for larger values of n.

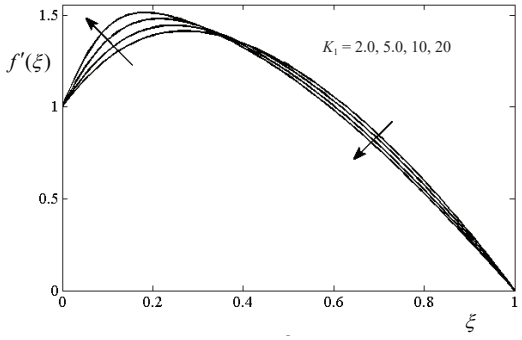

Figure 2. Variation in velocity profile $f'(\xi)$ for K_1 when $n=1.5$, M = 1.5, We = 0.2, and Re = 3.0

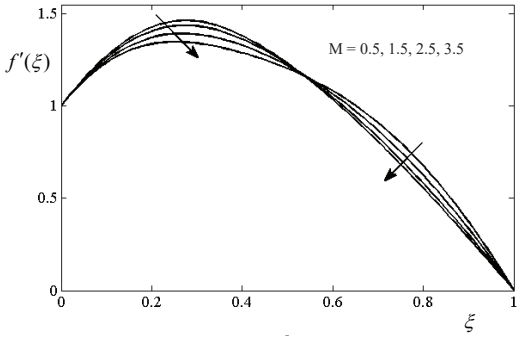

Figure 3. Variation in velocity profile $f'(\xi)$ for M when $K_1=5$, $n=1.5$, We = 0.5, and Re = 5

The analysis in pressure distribution $P(\xi)$ for diverge value of magnetic parameter and Reynolds number is displayed in fig. 7. The pressure field is decreased for higher values of Reynolds number, on the other hand, it enhances for higher values of magnetic parameter. Variation of pressure distribution $P(\xi)$ with Weand K_1 is illustrated in fig. 8. Pressure distribution decays gradually when the values of K_1 is increased, whilst, the pressure enhanced for larger values of Weissenburg number.

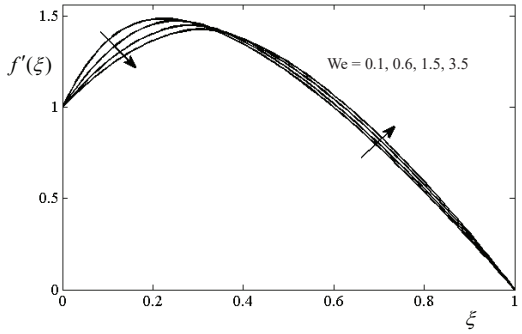

Figure 4. Variation in velocity profile $f'(\xi)$ for We when $K_1 = 5$, $n = 1.5$, M = 0.5, and Re = 4

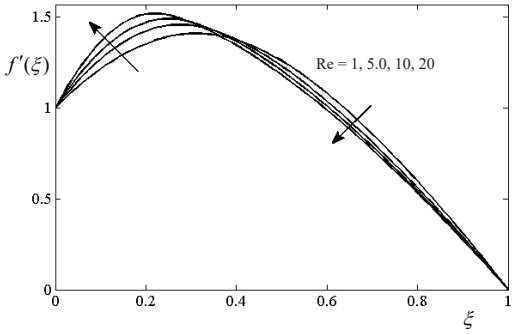

Figure 5. Variation in velocity profile $f'(\xi)$ for Re when $K_1 = 2$, $n = 1.5$, M = 0.8, and We = 0.4

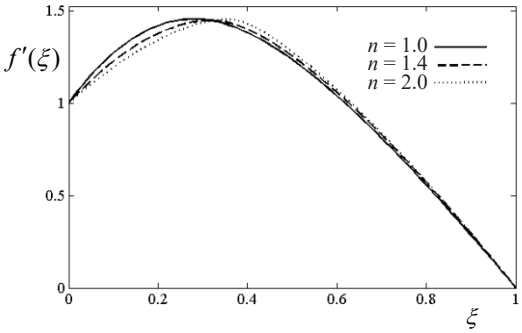

Figure 6. Variation in velocity profile $f'(\xi)$ for n when $K_1 = 2$, We = 1.0, M = 0.7, and Re = 4

Description of the Weissenberg number on the temperature distribution $\theta(\xi)$ is illustrated in fig. 9. One can observed that temperature and also the thermal boundary-layer thickness decreases for larger values of Weissenberg number. Analysis of radiation parameter Rd and Reynolds number on $\theta(\xi)$ is displayed in fig. 10. Decay in temperature distribution is observed for high values of Rd and Reynolds number. Impacts of Prandtl number and two values of convective parameter β on $\theta(\xi)$ is illustrated in fig 11. Higher values of Prandtl number and β is responsible for decay in the temperature field and also decreases the thermal boundary-layer thickness. Influence of temperature parameter θ_w on the $\theta(\xi)$ is presented in fig 12. High values of θ_w results in the enhancement of temperature field an in thermal boundary-layer thickness. One can also observed from this figure that for lower values of θ_w, non-linear thermal Rosseland approximation tends to behave as a Rosseland approximation but for larger value of θ_w, the temperature field turned to broader and S-shaped as investigate by Pantokratoras and Fang [8].

The analysis in skin friction coefficient $\mathrm{Re}_x^{1/2} C_f$ for various value of K_1 *vs.* Weissenburg number is illustrated in fig. 13. It is evident from this figure that the magnitude of $\mathrm{Re}_x^{1/2} C_f$

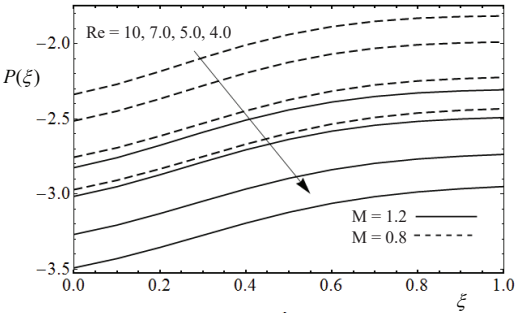

Figure 7. Variation in pressure profile $P(\xi)$ for M and Re when $n = 2.0$, We = 0.2, and $K_1 = 2$

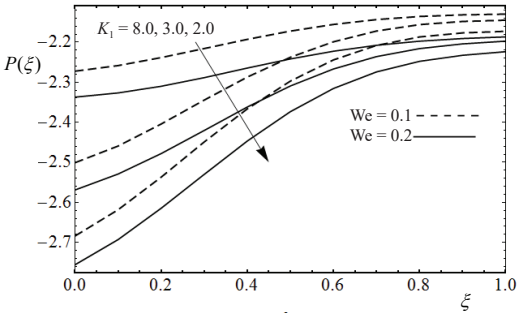

Figure 8. Variation in pressure profile $P(\xi)$ for We and K_1 when $n = 2.0$, M = 0.8, and Re = 5.0

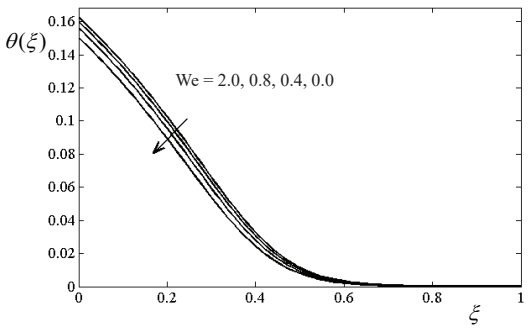

Figure 9. Variation in temperature profile $\theta(\xi)$ for We when $K_1 = 5$, M = 1.0, Re = 4, $\beta = 0.3$, Pr = 10, $n = 2$, $Rd = 1$, and $\theta_w = 7$

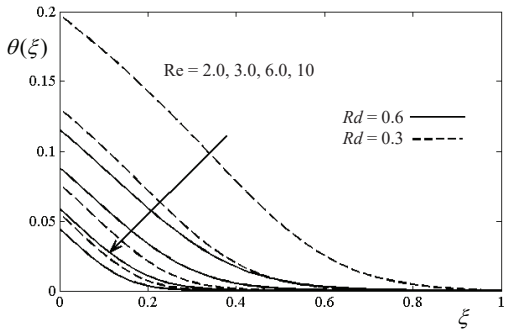

Figure 10. Variation in temperature profile $\theta(\xi)$ for Re and Rd when $K_1 = 2$, We = 1.0, M = 1.0, Pr = 10, $n = 2$, $\beta = 0.3$, and $\theta_w = 7$

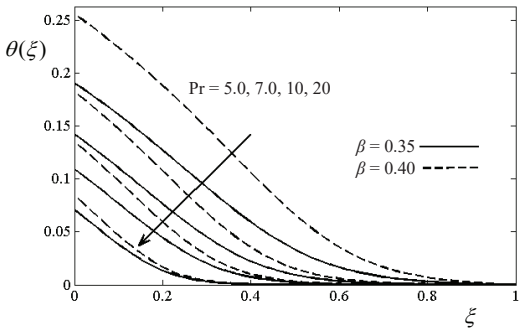

Figure 11. Variation in temperature profile $\theta(\xi)$ for Pr and β when $K_1 = 2$, We = 1.0, M = 1.0, Re = 5, $n = 2$, $Rd = 0.3$, and $\theta_w = 7$

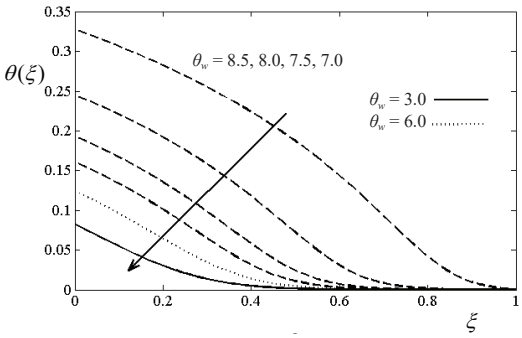

Figure 12. Variation in temperature profile $\theta(\xi)$ for θ_w when $K_1 = 5$, We = M = Rd = 1.0, $n = 2$, Pr = 10, $\beta = 0.3$, and We = 1

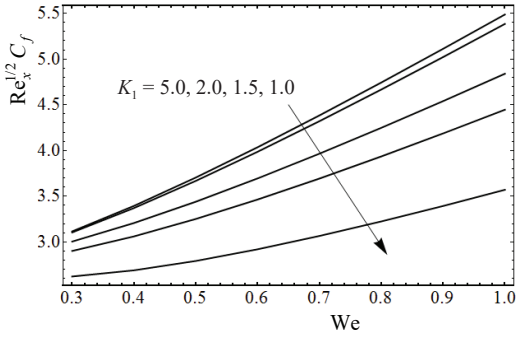

Figure 13. Variation of $\mathrm{Re}_x^{1/2} C_f$ for K_1 *vs.* We when Re = 3, $n = 2$, and M = 0.5

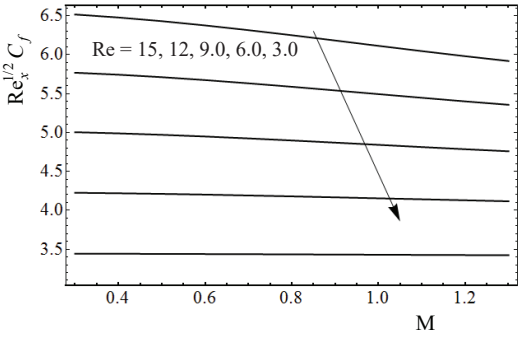

Figure 14. Variation of $\mathrm{Re}_x^{1/2} C_f$ for Re *vs.* M when We = 0.5, $K_1 = 2.0$, and $n = 2$

enhances for higher values of Weissenburg number and K_1. Figure 14 shows the analysis of $\mathrm{Re}_x^{1/2} C_f$ for various values of Reynolds number *vs.* magnetic parameter. The absolute values of $\mathrm{Re}_x^{1/2} C_f$ enhances for lager values of magnetic parameter and Reynolds number.

Table 1 indicates the numerical values of the local Nusselt number $\mathrm{Re}_x^{-1/2}\mathrm{Nu}_x$ for several values of $K_1, \mathrm{Re}, Rd, \mathrm{Pr}, \theta_w, \beta$ and by keeping $\mathrm{M}=1$, $\mathrm{We}=0.5$, and $n=2$ fixed. It is found that the magnitude of the $\mathrm{Re}_x^{-1/2}\mathrm{Nu}_x$ is increased by increasing the values of $\mathrm{Re}, Rd, \mathrm{Pr}, \theta_w$ and β, but it has the opposite trend for K_1.

Table 1. Numerical values of the Nusselt number $\mathrm{Re}_x^{-1/2}\mathrm{Nu}_x$ for various values of $K_1, \mathrm{Re}, Rd, \mathrm{Pr}, \theta_w$ and β by keeping $\mathrm{M}=1$, $\mathrm{We}=0.5$ and $n=2$ fixed

K_1	Re	Pr	Rd	θ_w	β	$\mathrm{Re}_x^{-1/2}\mathrm{Nu}_x$
1	3	7	0.5	2	0.2	0.94390
3						0.94158
5						0.94107
2	5					0.95438
	7					0.96102
	9					0.96537
	3	5				0.93267
		10				0.95087
		15				0.95919
		7	0.8			1.38579
			1.2			1.97010
			1.5			2.40371
			0.5	1.5		0.50701
				2.5		1.65850
				3		2.72500
				2	0.4	1.77350
					0.6	2.50157
					0.8	3.13451

Concluding remarks

In current analysis, we have investigated the characteristic of flow of a Carreau fluid in a semi permeable curved shape channel which is highly affected by the influence of magnetic field and non-linear radiative heat transfer with convective boundary condition. The solutions of governing flow equation are numerically computed for the fluid velocity and temperature distribution with the help of shooting method. The fundamental outcomes of the current study are.

- The velocity of fluid is increased with an increment in the values of Weissenburg number and Reynolds number, whilst it decreases for larger value of magnetic parameter and K_1.
- The temperature of the fluid and also the thermal boundary-layer thickness, shows decreasing behavior for higher values of Reynolds and Prandtl numbers.
- It is noticed that for high values of θ_w the temperature and also the thermal boundary-layer thickness shows increasing behavior. However, it decreases for higher values of Rd.
- For larger values of Reynolds number and K_1 the pressure distribution $P(\bar{\xi})$ shows decreasing behavior.

Acknowledgment

We are thankful to the reviewers for their encouraging comments and constructive suggestions to improve the quality of the manuscript.

References

[1] Berman, A. S., Laminar Flow in Channel with Porous Walls, *J. Appl. Phys*., *24* (1953), pp. 1232-1235
[2] Hayat, T., Abbas, Z., Heat Transfer Analysis on the MHD Flow of a Second Grade Fluid in a Channel with Porous Medium, *Chaos, Solut. Frac., 38* (2008), 2, pp. 556-567
[3] Kumar. J. P., *et al.*, Fully Developed Force Convective Flow of a Micropolar and Viscous Fluids in a Vertical Channel, *Appl. Maths. Modell*., *34* (2010), 5, pp. 1175-1186
[4] Sajid. M., *et al.*, Homotopy Analysis for Boundary Layer Flow of a Micropolar Fluid Through a Porous Channel, *Appl. Maths. Modell*., *33* (2009), 11, pp. 4120-4125
[5] Rassoulinejad-Mousavi, S. M., *et al.*, Heat Transfer Through a Porous Saturated Channel With Permeable Walls Using Two Equations Energy Model, *J. Porous Med., 16* (2013), 3, pp. 241-254
[6] Sheikholeslami, M., *et al.*, Analytical Investigation of MHD Nano Fluid Flow in a Semi Porous Channel, *Powd. Tech., 246* (2013), Sept., pp. 327-336
[7] Hatami, M., *et al.*, Nanofluid Flow and Heat Transfer in an Asymmetric Porous Channel with Expanding or Contracting Wall, *J. Molec. Liqu*., *195* (2014), July, pp. 230-239
[8] Pantokratoras, A., Fang, T., Sakiadis Flow with Nonlinear Rosseland Thermal Radiation, *Phys. Scrip.*, *87* (2012), 1, 015703
[9] Pantokratoras, A., Fang, T., Blasius Flow with Nonlinear Rosseland Thermal Radiation, *Meccanica, 49* (2014), 6, pp. 1539-1545
[10] Cortell, R., Fluid Flow and Radiative Nonlinear Heat Transfer Over a Stretching Sheet, J. *King Saud Uni. Sci*., *26* (2013), 2, pp. 161-167
[11] Kumar, K. G., *et al.*, Nonlinear Thermal Radiation Effect on Williamson Fluid with Particle Liquid Suspension Past a Stretching Surface, *Result in Physics*, *7* (2017), Aug., pp. 3196-3202
[12] Mustafa, M., *et al.*, Nonlinear Radiation Heat Transfer Effects in the Natural Convective Boundary Layer Flow of Nano Fluid Past a Vertical Plate: A Numerical Study, *Plos One*, *9* (2014), 9, pp. 1-10
[13] Kumar, K. G., *et al.*, Effect of Nonlinear Thermal Radiation on Double Diffusive Mixed Convection Boundary Layer Flow of Viscoelastic NanoFluid over a Stretching Sheet, *Int. J. Mech. Eng*., *12* (2017), Dec., 18
[14] Naveed, M., *et al.*, Thermophoresis and Brownian Effects on the Blasius Flow of a Nano Fluid Due to a Curved Surface with Thermal Radiation, *Eur. Phys. J. Plus*, *131* (2016), July, 214
[15] Hsiao, K. L., To Promote radiation Electrical MHD Activation Energy Thermal Extrusion Manufacturing System Efficiency by Using Carreau Nano Fluid with Parameters Control Method, *Energy, 130* (2017), July, pp. 486-499
[16] Hsiao, K. L., Combined Electrical MHD Heat Transfer Thermal Extrusion System Using Maxwell Fluid with radiative and Viscous Dissipation Effects, *Appl. Therm. Eng*., *112* (2017), Feb., pp. 1281-1288
[17] Rudraswamy, N. G., *et al.*, Combined Effect of Joule Heating and Viscous Dissipation on MHD Three Dimensonal Flow of a Jeffrey Nano Fluid, *J. NanoFluid*, *6* (2017), 2, pp. 311-317
[18] Kumar, K. G., *et al.* Influence of Nonlinear thermal Radiation and Viscous Dissipation on Three Dimensional Flow of Jeffrey Nanofluid Over a Stretching Sheet in the Presence of Joule Heating, *Nonlinear Eng*., *6* (2016), 3, pp. 207-219
[19] Abbas, Z., *et al.*, Hydromagnetic Slip Flow of Naofluid Over a Curved Stretching Surface with Heat Generation and Thermal Radiation, *J. Molec. Liq*., *215* (2016), Mar., pp. 756-762
[20] Hsiao, K. L., Stagnation Electrical MHD Nanofluid Mixed Convection with Slip Boundary on a Stretching Sheet, *Appl. Therm. Eng*., *98* (2016), Apr., pp. 850-861
[21] Hsiao, K. L., Corrigendum to Stagnation Electrical MHD Nanofluid Mixed Convection With Slip Boundary on a Stretching Sheet [*Appl. Therm. Eng*., *98* (2016), pp. 850-86], *Appl. Therm. Eng*., *125* (2017), Oct., p. 1577
[22] Kumar, K. G., *et al.*, Radiative Heat Transfer of Carreau Fluid Over a Stretching Sheet With Fluid Particle Suspension and Temperature Jump, *Results in Physics*, *7* (2017), pp. 3976-3983
[23] Makinde, O. D., Effect of Nonlinear Thermal Radiation on MHD Boundary Layer Flow and Melting Heat Transfer of Micropolar Fluid Over a Stretching Surface with Fluid Particle Suspension, *Defect Diffusion Forum*, *378* (2017), Sept., pp. 125-136
[24] Capobianchi, M., Aziz. A., Laminar Natural Convection From an Isothermal Vertical Surface to Pseudoplastic and Dilatant fluid, *ASME J. Heat Transf., 134* (2012),12, 122502
[25] Carreau, P. J., Rheological Equations From Molecular Network Theories, *Trans. Soc. Rheol*., *16* (1972), pp. 99-127

[26] Misra, J., *et al.*, Flow and Heat Transfer of a MHD Viscoelastic Fluid in a Channel With Stretching Wall: Some Applications to Haemodynamics, *Comp. Fluid*, *37* (2008), 1, pp. 1-11
[27] Hsiao, K. L., Micropolar Nanofluid Flow with MHD and Viscous Dissipation Effects Towards a Stretching Sheet With Multimedia Feature, *Int. J. Heat Mass Trasnf., 112* (2017), Sept., pp. 983-990
[28] Hayat, T., *et al.*, Radiation Effects on MHD Flow of Maxwell Fluid in a Channel with Porous Mesium, *Int. J. Heat Transf., 54* (2011), 4, pp. 854-862
[29] Raftrari, B., Vajravelu, K., Homotopy Analysis Method for MHD Viscoeleastic Fluid Flow and Heat Transfer in a Channel with a Stretching Wall, *Commun. Nonlinr. Sci. Simul*., *17* (2012), 11, pp. 4149-4162
[30] Abbas, Z., *et al.*, Chemically Reactive Hydromagnetic Flow of a Second Grade Fluid in a Semi Porous Channel, *J. Appl. Tech. Phys., 56* (2015), 5, pp. 878-888
[31] Masood, K., Magnetohydrodynamic Flow of Carreau Fluid Over a Convectively Heated Surface in the Presence of Non Linear radiation, *J. Magnetism Magnetic Material*, *412* (2016), Aug., pp. 63-68
[32] Khuri, A., Stokes Flow in Curved Channel, *J. Comput. Appl. Maths*., *187* (2006), 2, pp. 171-191
[33] Fu, Wu-S., *et al.*, Effects of a Porous Medium on Forced Convectyion of a Reciprocating Curved Channel, *Int. Commun. Heat Mass Transf*., *58* (2014), Nov., pp. 63-67
[34] Naveed, M., Flow and Heat Transfer in a Semi Porous Curved Channel with Radiation and Porosity Effects, *J. Porous Media*, *19* (2016), 5, pp. 1-11
[35] Abbas, Z., *et al.*, Nonlinear Radiative Heat Transfer and Hall Effects on a Viscous Fluid in a Semi Porous Curved Channel, *AIP Advanes*, *5* (2015), 10, 107124
[36] Sajid, M., *et al.*, Joule Heating and Magnetohydrodynamics effects on Ferrofluid Flow in a Semi Porous Curved Channel, *J. Molec. Liquid*, *222* (2016), Oct., pp. 1115-1120
[37] Rosseland, S., *Astrophysik und Atom Theoretische Grundlagen*, Springer Verlag, Berlin, 1931, pp. 41-44

Paper submitted: October 11, 2017
Paper revised: January 21, 2018
Paper accepted: February 3, 2018